Measuring Diameters of Rod-Shaped Bacteria in Vivo with Polarized Light Scattering

Burt V. Bronk,* Stephen D. Druger,‡ József Czégé,§ and Willem P. Van De Merwe§
*U. S. Air Force Project Reliance at ERDEC, Aberdeen Proving Ground, Maryland 21010-5423; ‡Department of Physics and Astronomy, Northwestern University, Evanston, Illinois 60208-3112; and §Biomedical Instrumentation Center, Uniformed Services University of the Health Sciences (USUHS), Bethesda, Maryland 20814-4799 USA

ABSTRACT The angular function for elements of the Mueller matrix for polarized light scattering from suspensions of microorganisms is known to be reproducible for different growths of a given bacterial strain in the log (or exponential) phase of growth. The reason for this, the stability of the size and shape distribution for cells, is briefly discussed. Experiments were performed using suspensions of two different strains of *Escherichia coli* cells in log phase and measuring the angular dependence of the Mueller matrix ratio $S34/S11$. Calculations were then performed using the coupled dipole approximation to model electromagnetic scattering from particles where the shape of an individual cell was approximated by a cylinder capped with hemispheres of the same radius as the cylinder. Using previously measured values for the length distribution and index of refraction of the cells, the calculated scattering curve was found to fit the measured curve very well. The values obtained for the cell diameters were quite close to diameters previously measured by optical microscopy. Thus this method provides a rapid and convenient method for monitoring bacterial diameters in vivo even when there is an appreciable distribution of bacterial lengths in the population.

INTRODUCTION

The Stokes four-vector (**I**, **Q**, **U**, **V**) completely describes the state of a beam of polarized, unpolarized, or partially polarized light. The matrix connecting the incoming Stokes vector with the scattered vector in a scattering experiment is called the Mueller (Bohren and Huffman, 1983) or Stokes matrix. It became feasible to measure all elements of this matrix by carrying over from astronomy the technique of photoelastic modulation (Hunt and Huffman, 1973, 1974). Soon after this, the technique was shown to be applicable to biological cells in water suspension (Bickel et al., 1976).

During the past several years we have been looking at the angular dependence of various elements of the Mueller matrix for scattering of polarized light from suspensions of microorganisms. The matrix element $S11$ corresponds to the scattering function for the intensity of unpolarized light. It has long been known that the angular variation of $S11$ is dependent on particle size, with larger size particles showing more scattering in the forward direction.

The matrix element $S34$ is sensitive to relative phase changes of the components of scattered polarized light arising from interaction of the scattering light with the scatterer (e.g., microorganism or other particle). We have found it to be particularly sensitive to the growth conditions of microorganisms. We have concentrated our measurements on this matrix element with the actual measurements made on the ratio

$$(S34/S11)^{\forall} = (S34 + S13)/(S11 + S14) \qquad (1)$$

The notation of Eq. 1 is used to indicate that for a spherically symmetric ensemble of scattering particles as is the case for randomly oriented cylindrically symmetric bacteria, the elements $S13$ and $S14$ may be neglected in this ratio (i.e., they are 0 if the symmetries are exact. We made measurements (not shown) that demonstrated these elements to be negligible for *Escherichia coli* bacteria.) Henceforth we refer to value of the ratio simply as $S34/S11$.

Using this ratio takes us into a range of values which, in our experiments, varies in magnitude between 0 and 3 %. This range is easier to deal with experimentally than the changes of several orders of magnitude that take place for the separate values of numerator and denominator as one varies angles between near forward and near back scattering. In previous presentations, we have shown that the measurements of this ratio are quantitatively reproducible (Van De Merwe et al., 1989) for a given strain of bacteria under carefully controlled growth conditions. For measurements on bacteria suspended in water, the ratio behaves as an oscillating function with increasing numbers of oscillations occurring as the size of the scattering particles increases. The main size dependence turns out to be strongly correlated with the diameter for rod-like cells (Bronk et al., 1992b) such as *E. coli*. We showed that this dependence could be qualitatively modeled using Mie scattering calculations from a distribution of spheres (Bronk et al., 1992a). In that case, a collection of spheres with a Gaussian distribution of diameters gave oscillating graphs with maxima and minima, which had similar locations to the experimental graphs; however, the shapes of the graphs differ somewhat from those obtained experimentally. In the present work we improve the correspondence between theory and experiment by using the coupled dipole calculation to model scattering from hemispherically capped cylinders, which

Received for publication 19 January 1995 and in final form 6 June 1995.
Address reprint requests to Dr. Burt V. Bronk, SCBRD-RT, Building E5951, ERDEC, Aberdeen Proving Ground, MD 21010-5423. Fax: 410-671-2742, E-mail: bvbronk@cbda7.apgea.army.mil.

0006-3495/95/09/1170/08 $2.00

closely resemble the microscopically observed shape of *E. coli* cells. In this case both the shapes of the calculated graphs and their peak locations correspond very closely to those obtained experimentally.

MATERIALS AND METHODS

We describe the experimental procedures elsewhere (Van De Merwe et al., 1989; Bronk et al., 1991, 1992a), so only a brief summary is given here. The main biological feature is to allow a pure strain of bacteria to grow for multiple generations at low density (optical density <0.1) in the given medium with aeration at 37°C so that a good approximation to an ideal log phase (i.e., exponential growth) size distribution is achieved. Cells were then prepared for the scattering experiment by spinning them down and then resuspending them at low density in 0.9% saline. Microscopic measurements giving the log phase length distribution and average diameters were made following the same preparation. The microscopic measurements were made by photographing the cells in saline through Zeiss phase contrast optics (Carl Zeiss, Oberkochen, Germany) with a 63× oil immersion lens with a 1.4 numerical aperture (Bronk et al., 1992b). Two different media were used in the present experiments. LB medium was used for growth of the *E. coli* K12 strain (American Type Culture Collection (ATCC, Rockville, MD) no. 49539), and M1 was used for growth of the *E. coli* B/r strain (ATCC 12407). The recipes for these media are standard (e.g., Bronk et al., 1992b).

The scattering measurements were made with a slight modification to the procedure previously described (Bronk et al., 1992a) in which various optical elements were used to obtain the desired combination of Mueller matrix elements. A lock-in amplifier is coupled with a photoelastic modulator that varies the polarization of the incoming light to improve signal-to-noise ratio for the rather small values measured. The photoelastic modulator consists of a mechanically vibrating optical element (a crystal acting as a variable retarder), which is resonant with the vibrations of a piezoelectric transducer at 50 kHz. The retardation varies as $A\sin(\omega t)$ where ω is 2π times the resonant frequency and A is chosen as the first zero of the zeroth order Bessel function (see Bohren and Huffman, 1983, p. 418). This retardation causes the polarization of the beam to vary (approximately) between left and right circular polarization at the same frequency. Additional optical elements between the scatterer and the phototube cause a portion of the light signal to vary in phase with the polarization and proportionally to particular Mueller matrix elements. The lock-in amplifier is tuned to the signal and acts as a narrow pass filter measuring the AC (50 kHz) part of the signal coming from the photomultiplier tube, and converts it into a DC output. This output is digitized (e.g., as the Y input), as is the scattering angle (i.e., the angle of the arm to the phototube with the forward direction of the laser). A detailed description and diagram of the apparatus and the physics involved, as well as listings of papers pioneering the method by Hunt, Huffman and collaborators are given in the Bohren and Huffman book (1983) and in the chapter by Bronk et al. (1992a).

The only modifications made for the present experiments were to digitize measurements and to immerse the cuvette in a larger diameter vessel (~7 cm), which was filled with water to provide a somewhat closer match to the refractive index of the cuvette and the buffer inside. This makes it easier to eliminate undesired reflections from the cuvette and to image the output scattered light on a pinhole near the phototube. Measurements were taken at 1° intervals, and the angular resolution is slightly better than 1°. (Mineral oil could be used to give an even better match of refractive indices with the glass, but we found water was adequate and more convenient). A photomultiplier tube is rotated around the cuvette containing the scatterers at a distance of ~30 cm from the center, and the signal is recorded at various angles with a time average taken over 1 s at each measurement point. A diode laser (Melles Griot) emitting at 670 nm with ~2 mm diameter beam through the cuvette provided the scattering light. About 2–4 ml sample suspension was held in a circular quartz cuvette with a 5 mm flat face toward the laser. We focused the scattered light from ~1.5 mm diameter, giving an active volume of about 3.5×10^{-3} ml. Our suspensions had ~$2–5 \times 10^6$ bacteria/ml so that scattering from $1–2 \times 10^4$ bacteria was averaged during each second-long measurement. Because the bacteria were immersed in water, a wavelength of 502.6 nm was used for the calculations. A relative refractive index of 1.03, which is typical for these bacteria (Barer, 1956), was used. Absorption, which is extremely small at this wavelength, was ignored. All scattering experiments were performed with optical density <0.1 at 600 nm. Previous experiments indicated that only single scattering occurs at this density (Van De Merwe et al., 1989; Bronk et al., 1992a).

Bacterial populations

The scattering function ($S34/S11$) is quite sensitive to small changes in size of the scattering particles, and the bacteria in a growing population are distributed over a substantial range of sizes. Nevertheless, in an earlier study (Van De Merwe et al., 1989), we were able to show that the angular graph of $S34/S11$ for a particular bacterial strain is quite reproducible when a carefully prepared log phase population is utilized for the experiments. Those experiments were done for separate growths of the same bacteria in separate labs with the measurements made on somewhat different instruments. The reason for this reproducibility is the well known, but still remarkable fact that the size distribution for cells growing at low density in log phase suspension is quite stable and reproducible for specified growth conditions. We therefore give a brief heuristic discussion of the origin of this stable size distribution.

In any bacterial population growing freely for several generations, the measurable parameters of individual cells vary broadly. Consider the relatively simple case of cell volumes. It is known that the interdivision time (Kubitschek, 1962) and the relative size (Trueba et al., 1982) of two daughter cells after mitosis both have random character. Hence, even if an ensemble of cells were somehow selected to have nearly uniform values for volume and age-in-cycle (age), the cell parameters would again be distributed rather broadly between a maximum and minimum value after just a few generations (Bronk et al., 1968). However, with a little care, conditions can be achieved such that the distribution of ages and hence size quickly approach a reproducible asymptotic function (Bronk, 1980; Bronk et al., 1968, 1974).

Many types of bacteria may be grown with a well defined and identical environment for every cell of the population. The genetic material determining response to given conditions is identical (except for rare mutations) for each cell of a clone. After several generations of growth under such well defined conditions, it is a reasonable hypothesis that the values for any measurable parameter of the living cells will approach some quantitatively reproducible distribution. The conditions of growth can most easily be kept essentially identical for many generations when the individual cells are well separated spatially as in a dilute suspension (or under crowded conditions in a chemostat). This hypothesis has been verified theoretically for the age distribution (Bronk et al., 1968) and experimentally for the volume distribution of some bacteria (Trueba et al., 1982).

It is straightforward to show that the age distribution for log-phase cells will approach

$$g(z) = \exp(-\alpha z)(1 - F(z)) \tag{2}$$

with z the age of a cell since it appeared at division, $\alpha = \ln(2)/T_c$, with T_c the mean time between divisions and

$$F(z) = \int_0^z f(z')\, dZ' \tag{3}$$

where $f(z')\, dz'$ is the probability that a newly divided cell will divide again after a time in the interval near z'. Kubitschek (1962) gave strong evidence that the distribution of division rates (i.e., the reciprocal of division times)

is well described by a Gaussian. In this case, the probability for a cell to have division time near z is given by

$$f(z)\,dz = (C/z^2)\exp(-(z - z_0)^2/2(\sigma_\kappa z_0 z)^2)\,dz \qquad (4)$$

with C the normalization constant. While the distribution given by Eq. 4 does not possess a well defined mean or variance, it is easy to see specific examples in which the resulting age distribution is hardly distinguishable from one that results from a Gaussian distribution of interdivision *times*.

We may relate the size of a cell to its age as follows. Define $P(v|z)$ as the probability that a cell of age in cycle z is of volume v; then it follows that

$$P(v) = \int_0^\infty P(v|z)\,g(z)\,dz \qquad (5)$$

is the probability density function for an individual cell to have volume in the neighborhood of volume, v. If the physical conditions of growth are precisely defined and identical for each cell, then $P(v)$ is a unique function for a particular strain of bacteria brought to log phase under those growth conditions. These idealized conditions are well approximated when the bacteria have been growing in log phase at low density for many generations.

For some time it has been known that *E. coli* cells grow primarily by extending their length with very little change in diameter under constant growth conditions (Marr et al., 1966). Our microscope measurements (not shown) corroborate this and show clearly that there is little significant correlation of diameter with length changes during the cell cycle for these bacteria under the conditions of these experiments. (It is likely that most of the observed variation in diameter is due to the experimental error caused by limitations of light microscopy.) Electron microscopy (EM) provides orders of magnitude better resolution; however, it requires extensive preparation during which bacterial volumes are known to shrink by as much as 50%, so that the uncertainties for EM measurements are even greater than those for optical microscopy.

In Fig. 1 we present histograms summarizing microscopic measurements of length for log phase populations of the two strains of *E. coli* used in the present study. Each strain was measured in a steady state log phase growth in its respective medium as indicated in the figure caption (Bronk et al., 1992a,b). Since growth of an individual cell is achieved by increasing its length, we expect that the histogram is a good approximation of a histogram calculated from the ideal function $P(v)$ from Eq. 5 and the assumption that $P(L) \equiv P(v)$. It appears similar to the "universal" graph obtained experimentally (Trueba et al., 1982) for several strains of *E. coli*.

Since the histograms of Fig. 1 were obtained under the same conditions as the scattering graphs to be studied, we made the assumption that the population percents for each size class are a sufficiently precise representation for the actual values in the scattering experiment (i.e., these are the values used in our model calculations).

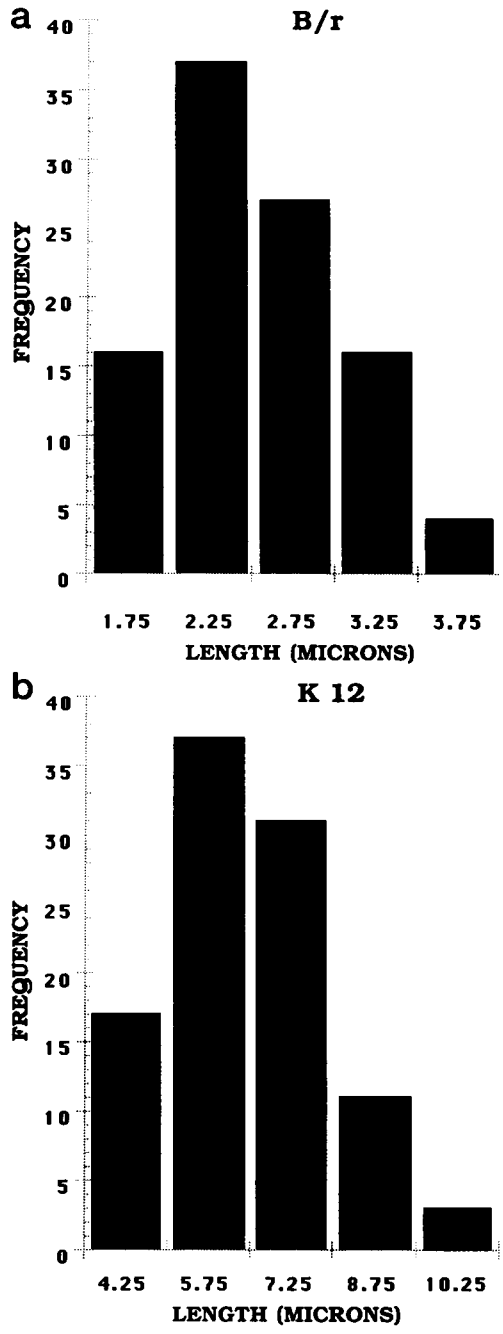

FIGURE 1 Histograms showing frequency of length of individual cells obtained from optical micrographs of bacteria grown in M1 minimal medium (B/r) or LB broth (K12). See Bronk et al. (1991).

Calculations

Calculations of electromagnetic scattering from particles of arbitrary shape may be accurately performed using the coupled dipole model (CDM). Scattering from a variety of targets has been studied with this model (Devoe, 1964, 1965; Purcell and Pennypacker, 1973; Druger et al., 1979; Draine, 1988). Recently Draine and collaborators extensively studied the properties of the model (Draine and Flatau, 1994; Flatau et al., 1993) in order to apply it to determine the effect of interstellar dust grains on celestial radiation.

The method models a dielectric particle in an applied incident field as an array of polarizable components (i.e., point electric dipoles) each with a polarizability α. The local field at each point dipole is the sum of the field of the incident applied field and the field of each of the other dipoles. We choose the points to lie on a simple cubic lattice. With N points used to fill the shape of the particle, this produces $3N$ linear equations for the three local field components at each dipole. The equations for the ith dipole are

$$\mathbf{P}_i = \alpha \mathbf{E}_i$$

$$\mathbf{E}_i = E_o \mathbf{e}_x \exp(ikz_i) + \sum_{j \neq 1} [\exp(ikr_{ij})/r_{ij}^3] \cdot [k^2(\mathbf{r}_{ij} \times \mathbf{P}_j) \qquad (6)$$

$$\times \mathbf{r}_{ij} + [(1 - ikr_{ij})/r_{ij}^2][3\mathbf{P}_j \cdot \mathbf{r}_{ij}\mathbf{r}_{ij} - r_{ij}^2 \mathbf{P}_j]\,]$$

where $\mathbf{E}_i$ and $\mathbf{P}_i$ are the vector field and polarizability at the ith dipole.

The polarizability, α, of the dipoles is determined in the present case from the dielectric constant or equivalently the known index of refraction relative to the medium (i.e., water in the present case) by means of the Clausius Mossotti relation,

$$(4\pi/3)\rho\alpha = (\epsilon - 1)/(\epsilon + 2) \quad (7)$$

with ρ the density of the dipoles.

The shape of *E. coli* cells as may be seen in many photographs is well represented by a cylinder capped on both ends by hemispheres of the same radius as the cylinder. A single representative size is specified by two parameters, length (L) and diameter (D). From these parameters we obtain the volume of the cell, and we next specify a desired approximate number of dipoles to be used in a particular calculation. From this and the cell volume, we obtain a volume per dipole and in turn an approximate length between dipoles placed at the vertices of a cubic lattice. We then align the cylinder axis along the (0,0,1) axis within the lattice. This assures a uniform effective diameter for the cylinder. We then test each dipole to see whether it was inside the capped cylinder, discarding those that are not. We readjust the lattice spacing, if necessary, to be consistent with the dimensioning of the program. For a typical case we start with 1000 dipoles to model a bacterium with L = 2.5 μm, D = 1 μm, and wavelength of the scattering light = ~500 nm. The spacing between dipoles will be ~0.12 μm. This gives an uncertainty at the edge of the shape approximated of ~0.06 μm. The model was tested against a calculation based on the exact Mie formula for a sphere and gave a good approximation for $S34/S11$ for a 1 μm sphere for $\theta < -140°$C when 739 dipoles were used in the model calculation (results not shown). The bacteria are assumed to be randomly oriented in the suspension used for the scattering experiments. Thus the scattering calculation must be averaged over random orientations of the capped cylinders. The z direction is defined as the propagation direction for the incoming laser light, the positive y direction is at 90°C in a horizontal plane formed by it and the z axis. The axes are right-handed with x pointing up. θ is defined as the angle from z in the zy plane. After a θ rotation of the cylinder about the laboratory x axis, ϕ defines a further rotation about the laboratory z axis. A third rotation about the body axis of the cylinder is neglected, since cylindrical symmetry is approached as the number of dipoles increases. This is verified for our calculation by the fact that the graph of $S34/S11$ is a good approximation of the graph of $(S34/S11)^{\frac{1}{2}}$. We believe that departures from cylindrical symmetry due to the discreteness of the model are smoothed over since we further average over ~16 different sizes, which should randomly average over departures from that symmetry. The angular averages are made over ~50 different orientations spread uniformly over 4 π steradians and were checked in particular cases with averages over many more orientations. The averaging is done with a Simpson's rule integration over θ and ϕ.

RESULTS

The results of two calculations using the CDM for a single sphere are compared with the numerical calculation using the exact Mie solution in Fig. 2. The graph of $S34/S11$ versus angle obtained with the CDM is quite similar to that obtained with the exact solution. The sharp extrema are features that other calculations determined to be washed out when the scattering was from an ensemble of spheres of different sizes.

In Fig. 3 we present the results of a calculation made for three single orientations of a capped cylinder with its parameters close to those that are appropriate for one of our experiments. These graphs are not very similar to those obtained with random orientations and a distribution of different bacterial sizes as in the experimental observations (see below). The graphs of Fig. 3 have much more detailed structure with sharper and higher individual peaks, which suggest future experiments with oriented rod-shaped bacteria.

In another set of calculations we compared graphs of $S34/S11$ obtained from the CDM calculations for capped cylinders of three different lengths, 4.0, 6.0, and 8.0 μm, but

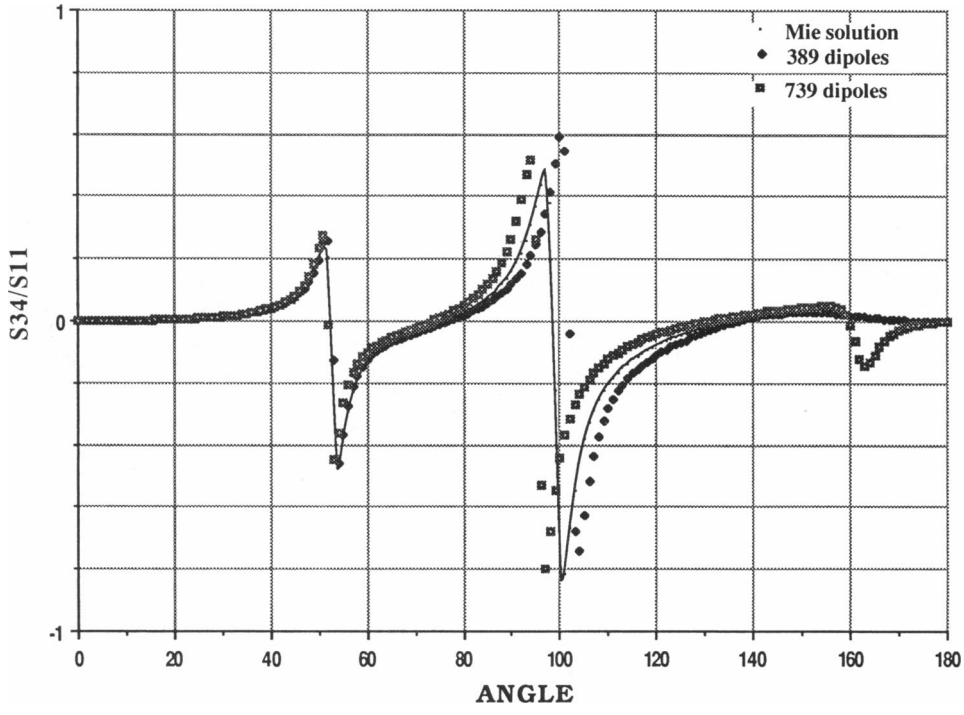

FIGURE 2 Calculations comparing graph of $S34/S11$ versus angle obtained from Mie solution with those obtained from the CDM. All calculations are for single sphere with radius = 0.5 μm, refractive index = 1.03 + 0.0i and scattering wavelength = 633 nm.

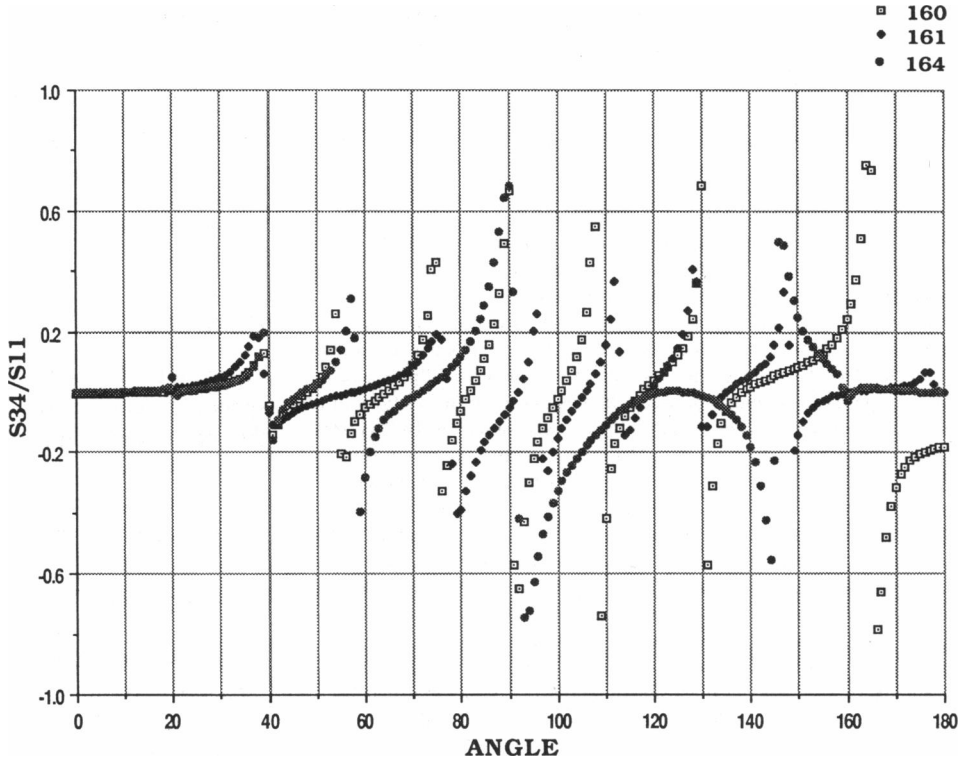

FIGURE 3 *S34/S11* graph calculated with CDM for capped cylinder of length 2.25 μm and diameter 0.9 μm, and various fixed orientations with respect to the incoming laser light. (□) Run 160; $\theta = 45°$, $\phi = 0°$. (♦) Run 161; $\theta = 45°$, $\phi = 45°$. (●) Run 164; $\theta = 90°$, $\phi = 45°$. Wavelength used for calculations is 502.6 nm as in the experiments.

of the same diameter, 1.73 μm. The three graphs obtained after averaging over the entire 4π sphere of orientation angles are shown in Fig. 4. We note that there is some difference in shape between the graphs for different length bacteria, but that the locations of maxima and minima obtained for different lengths are about the same for angles $<120°$. This is in agreement with earlier experimental results (Bronk et al., 1992b), which showed a strong correlation of peak location with diameter of rod-shaped bacteria, but no correlation of peak location with average length of the cells.

The shapes of the graphs of Fig. 4 still have sharp triangular peaks, unlike what is observed experimentally, and reach significantly higher peaks than in the experimental case. This is because a single size was used for each graph, whereas in the experiments we used a distribution of

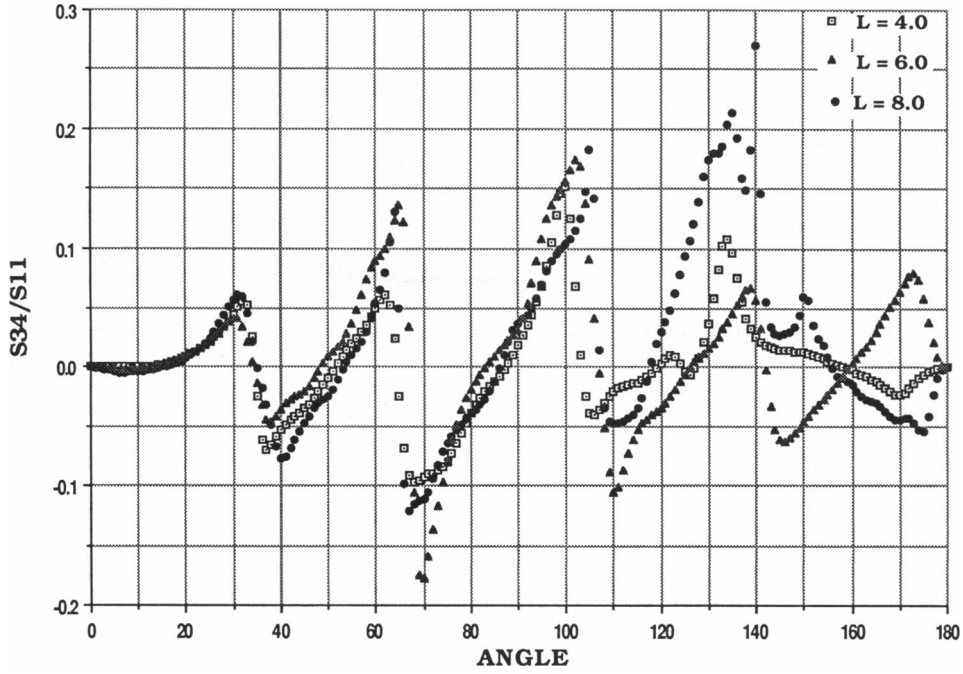

FIGURE 4 Rotationally averaged graph of *S34/S11* for single-sized capped cylindrical bacteria of lengths 4,0, 6.0, and 8.0 μm but all of diameter 1.34 μm calculated with the CDM. Scattering wavelength is 633 nm.

sizes. When size averaging was performed with the results of the CDM model calculations we obtained smoothed graphs resembling the experimental results.

We used the following procedure to apply the model to experimental data. First we constructed individual graphs from an average over angles for a given size capped cylinder. These graphs were then averaged over the four most important categories in the appropriate length histogram shown in Fig. 1. This was done for various diameters in size steps of 0.05 μm. Then we studied graphs obtained using various combinations of diameters for the closest match to the experimental data. The resultant fits to data are shown in Fig. 5 for the two different bacterial strains. We used a simple four-category Gaussian-like distribution of diameters to obtain the calculated graph. The diameter distributions used are shown in Fig. 6. We allowed only one other free parameter; a scaling factor of $\sim$½ was applied to make the calculated graph more closely resemble the experimentally measured one. Other calculations (not shown) indicated that averaging over more size categories reduces the size of the peaks. The requirement for a scaling factor indicates simply that a distribution with a larger number of size categories more closely approximates the experimental population.

In Table 1 we give a comparison of diameters (D) obtained from the present scattering measurements with in

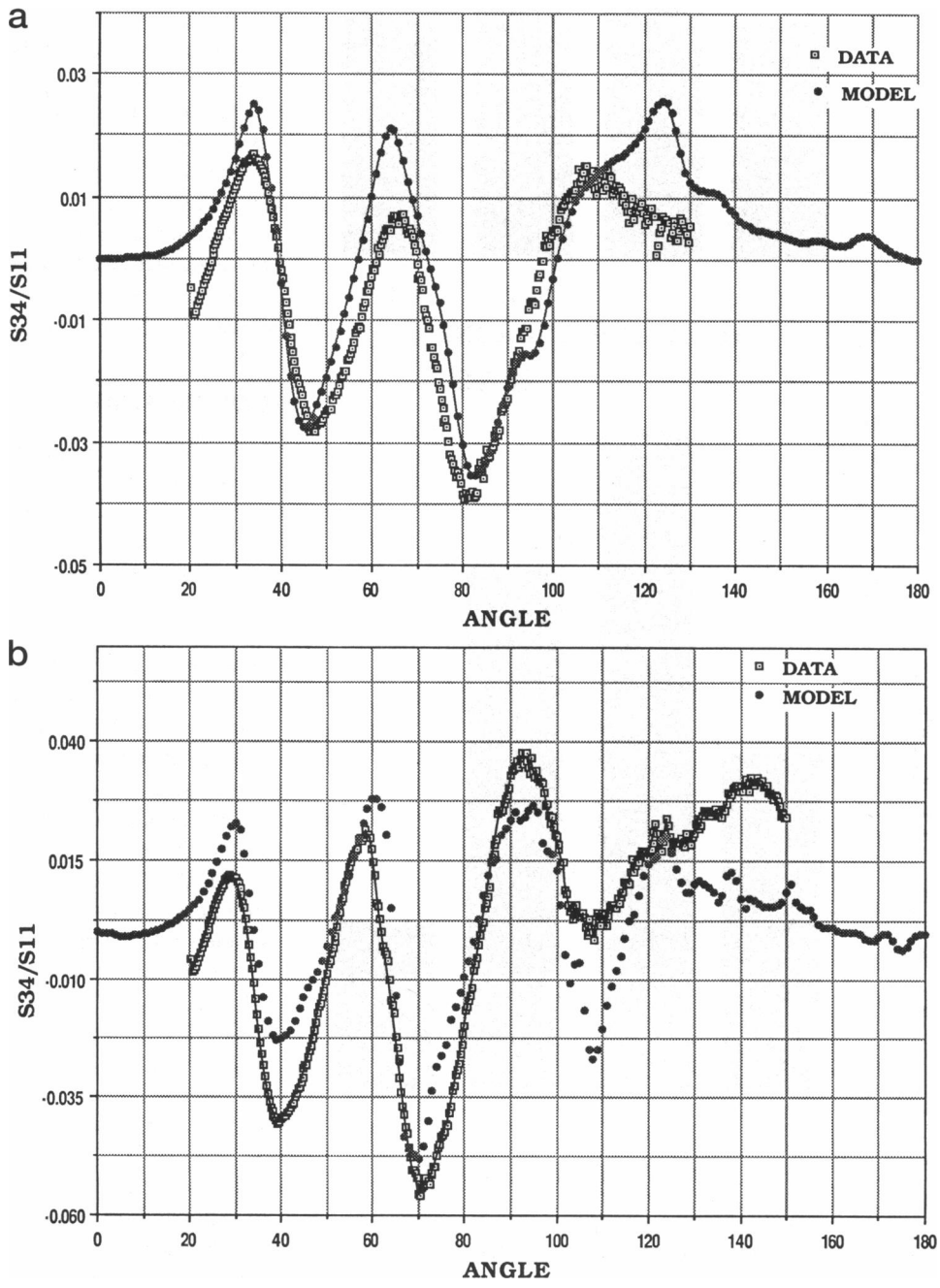

FIGURE 5 (*a*) $S34/S11$ versus angle for experimental data from log-phase *E. coli* B/r. (□) Data; (●) Model. (*b*) Same for *E. coli* K12. Scattering wavelength is 502.6 nm.

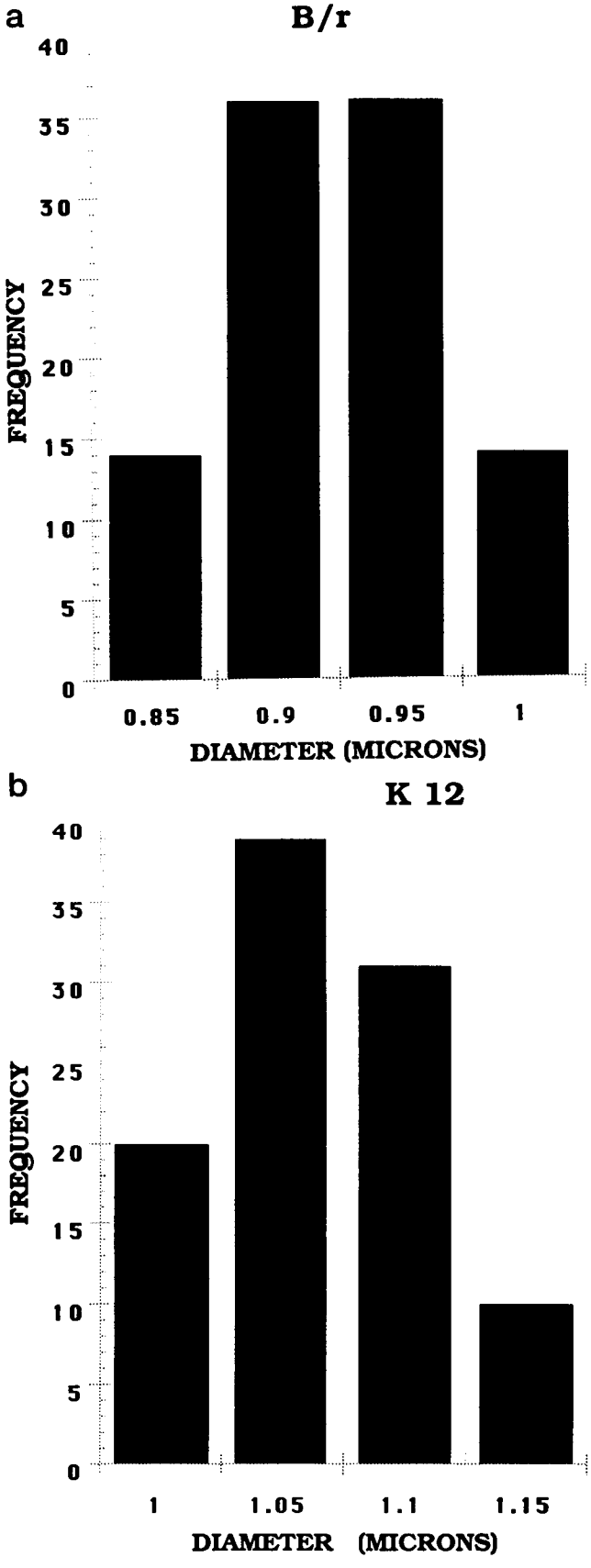

FIGURE 6 Histograms showing distribution of diameters of individual cells assumed to obtain fit of Fig. 5, (*a*) for *E. coli* B/r, and (*b*) for *E. coli* K12

TABLE 1

	E. coli strain	
Parameters	B/r	K12
D scattering	0.92 ± 0.04	1.055 ± 0.07
D microscopy	0.78 ± 0.11	1.15 ± 0.10

D, diameter.

vivo microscopic measurements made under the same conditions. Comparing figures in the column for each strain shows that a very satisfactory agreement of the results has been achieved with the two very different measurements. The errors indicated are standard deviations of the microscopic measurements or of the histograms used in the fit to scattering. A more conservative estimate of the uncertainty for the present state of the model is ~0.1 μm in the diameter because of the limitation on the accuracy of "stuffing" the cell shape with dipoles. This is at least as good as what is available from optical microscopy. Necessary deformation of the cells during preparation for EM would lead to even larger errors. The sensitivity of the scattering measurements at this point is somewhat better than 50 nm. We could model to this sensitivity by increasing the number of dipoles by a factor of ~8–10, but this would increase the time of the calculation by a large factor.

CONCLUSIONS

It is satisfying that most of the complicated qualitative and quantitative features of the experimental data are reproduced quite satisfactorily for angles <130°. As is well known, back scattering is much more sensitive to details of the model and further refinement of the model would be required to establish its applicability for larger angles. Potential sources of error for Mueller matrix measurements have been analyzed to some extent by Johnston et al. (1988). Error analysis of the instrumentation can be quite complicated when electro-optic elements are utilized for the measurements as in this study. Our conclusion is that it is more useful to estimate the uncertainty by comparing the results of measurements with those obtained from completely independent measurements with the same particles as was done here for bacterial diameters. The present measurements indicate agreement to about 10% with the microscopic studies. Other measurements (not shown) comparing diameters of latex beads calibrated with EM with those obtained with the methods used here indicate at least as good an agreement.

The angular variation of the $S11$ Mueller matrix element for light scattering has been utilized elsewhere to measure size and refractive index of bacteria and spores, which can be modeled by spheres (Wyatt, 1975; Ulanowski, 1987). The advantages of the present method are that the diameter for a population of rod-shaped cells can be measured rapidly in real time and in vivo with an average over many cells, and the diameter measurement can be separated from the

length measurement. This allows one to follow changes in average diameter of the cells during the course of an experiment.

There is a lively interest in microbiology in determining how bacteria are able to rapidly adjust their physical parameters to changing growth conditions. The bacteria start growing larger (Woldringh et al., 1980; Kubitschek, 1990) or smaller (Zaritsky and Helmstetter, 1992; Zaritsky et al., 1993) within a few minutes of a shift to a richer or poorer medium. The size measurements for such shift experiments are usually made either with optical microscopy, EM, or with a Coulter type counter sensitive to volume changes. Although cell length is measured very satisfactorily with optical microscopy, each of the methods is rather limited with respect to cell diameter, a very important parameter in the measurements. We believe that adding the present type of scattering measurement, along with its modeling, to the other measurements will stimulate many additional interesting experiments in which changes in diameter play an important role.

REFERENCES

Barer, R. 1956. Phase contrast, and interference microscopy in cytology. *In* Physical Techniques in Biological Research. G. Oster and A. W. Pollister, editors. Academic Press, New York.

Bickel, W. S., J. F. Davidson, D. R. Huffman, and R. Kilkson. 1976. Application of polarization effects in light scattering: a new biophysical tool, *Proc. Natl. Acad. Sci. USA.* 73:486–490.

Bohren, C. F., and D. R. Huffman. 1983. Absorption and scattering of light by small particles. Wiley, New York.

Bronk, B. V. 1980. Limitations on determinism at the cellular level in biology due to variability at the molecular level. *In* Applied Stochastic Processes. G. Adomian, editor. Academic Press, New York. 37–70.

Bronk, B., G. J. Dienes, J. Gautschi, and R. Schindler. 1974. Kinetic cell cycle analysis of a cultured mammalian cell Population. *Biophys. J.* 14:607–624.

Bronk, B., G. J. Dienes, and A. Paskin. 1968. The stochastic theory of cell proliferation. *Biophys. J.* 8:1353–1397.

Bronk, B. V., W. P. Van De Merwe, and D. R. Huffman. 1992a. Light scattering as a means for detecting subtle changes in microbial populations. *In* Modern Techniques for Rapid Microbiological Analysis. W. Nelson, editor. VCH Publishers, New York.

Bronk, B. V., W. Van De Merwe, and M. Stanley. 1991. Comparative Studies of Bacterial Shape, and Its Effect on the (S34/S11)* Angular Scattering Pattern, U. S. Army ERDEC Technical Report CRDEC-SP-036, Aberdeen Proving Ground, Maryland.

Bronk, B. V., W. P. Van De Merwe, and M. Stanley. 1992b. An in-vivo measure of average bacterial cell size from a polarized light scattering function. *Cytometry.* 13:155–162.

Devoe, H. 1964. Optical properties of molecular aggregates. I. Classical model of electronic absorption and refraction. *J. Chem. Phys.* 41: 293–400.

Devoe, H. 1965. Optical properties of molecular aggregates. II. Classical theory of refraction and absorption of solutions and crystals. *J. Chem. Phys.* 43:3199–3208.

Draine, B. T. 1988. Discrete dipole approximation and its application to interstellar graphite grains. *Astrophys. J.* 333:848–872.

Draine, B. T., and P. J. Flatau. 1994. Discrete dipole approximation for scattering calculations. *J. Opt. Soc. Am. A.* 11:1491–1499.

Druger, S. D., M. Kerker, D. S. Wang, and D. D. Cooke. 1979 Light scattering by inhomogeneous particles. *Appl. Optics.* 18:3888–3889.

Flatau, P. J., K. A. Fuller, and D. W. Nackowski. 1993. Scattering by two spheres in contact: comparisons between discrete-dipole approximation, and modal analysis. *Appl. Opt.* 32:3302–3305.

Hunt, A. J., and D. R. Huffman. 1973. A new polarization-modulated light scattering instrument. *Rev. Sci. Instrum.* 44:1753–1762.

Hunt, A. J., and D. R. Huffman. 1974. A polarization-modulated instrument for determining liquid aerosol properties. *Jpn. J. Appl. Phys.* 14(Suppl.):435–440.

Johnston, R. G., S. B. Singham, and G. C. Salzman. 1988. Polarized light scattering. Comments. *Mol. Cell. Biophys.* 5:171–192.

Kubitschek, H. E. 1962. Normal distribution of cell generation rate. *Exp. Cell Res.* 26:439–450.

Kubitschek, H. E. 1990. Cell volume increase in *E. coli* after shifts to richer media. *J. Bacteriol.* 172:94–101.

Marr, A. G., R. J. Harvey, and W. C. Trentini. 1966. Growth and division of *Escherichia coli*. *J. Bacteriol.* 91:2388–2389.

Purcell, E. M., and C. R. Pennypacker. 1973. Scattering and absorption of light by nonspherical dielectric grains. *Astrophys. J.* 186:705–714.

Trueba, F. J., O. M. Neijssel, and C. L. Woldringh. 1982. Generality of the growth kinetics of the average individual cell in different bacterial populations. *J. Bacteriol.* 150:1048–1055.

Ulanowski, Z., L. K. Ludlow, and W. M. Waites. 1987. Water content and size of spore components determined by laser diffractometry, *FEMS Microbiol. Lett.* 40:229–232.

Van de Merwe, W., D. Huffman, and B. Bronk. 1989. Reproducibility and sensitivity of polarized light scattering for distinguishing bacterial suspensions. *Appl. Opt.* 28:5052–5057.

Woldringh, C. L., N. B. Grover, R. F. Rosenberger, and A. Zaritsky. 1980. Dimensional rearrangement of rod-shaped bacteria following nutritional shift-up. *J. Theor. Biol.* 86:421–439, 441–454.

Wyatt, P. J. 1975. Observations on the structure of spores. *J. Appl. Bacteriol.* 38:47–51.

Zaritsky, A., and C. E. Helmstetter. 1992. Rate maintenance of cell division in *E. coli* B/r: analysis of a simple nutritional shift-down. *J. Bacteriol.* 174:8152–8155.

Zaritsky, A., C. L. Woldringh, C. E. Helmstetter, and N. B. Grover. 1993. Dimensional rearrangement of *E. coli* B/r cells during a nutritional shift-down. *J. Gen. Microbiol.* 139:2711–2714.